1J1-2

Effect of Acoustic Impedance Distribution and Histopathological Structure on Backscatter Coefficient Analysis of Skin Tissue

音響インピーダンス分布と組織構造が皮膚組織の後方散乱係数解析に与える影響

Masaaki Omura[1†], Kenji Yoshida[2], Shinsuke Akita[3], and Tadashi Yamaguchi[2*]
([1]Grad. School Sci. Eng., Chiba Univ.; [2]Center for Frontier Medical Engineering, Chiba Univ.; [3] Grad. School Med., Chiba Univ.)
大村 眞朗[1†], 吉田 憲司[2], 秋田 新介[3], 山口 匡[2*]
([1] 千葉大 院融合, [2] 千葉大 CFME, [3] 千葉大 院医)

1. Introduction

Skin lymphedema (LE) with middle severity has tissue properties such as inflammation, fibrosis, and edema. It is assumed that quantitative ultrasound parameters have different features related to different ultrasonic backscatter properties between without and with LE. Our previous studies indicated that the difference of the backscattering properties, e.g., backscatter coefficient (BSC), was obtained between without and with LE [1]. We aimed to clarify the relationship among backscattered signals, microscopic acoustic properties, and pathological structures to understand the effect of the differences in microscale collagen and elastin fibers for those in the macroscopic backscattering properties.

2. Materials and Methods

BSCs were calculated based on three spatial features of human skin samples as shown in **Fig. 1**.

2.1 Human samples

Collected samples were without LE [LE (−)] (n=5) and with LE [LE (+)] (n=5), and each tissue was excised from an abdomen and a thigh of women patients, respectively. Each sample was divided into two masses for the measurement and histopathological specimen. Each sample for the measurement was embedded within 3 wt% low-melting agarose at 40°C. After coagulation, the agarose phantom was sunk in the degassed water at 20°C.

2.2 Analysis of backscattered signals

RF echo signals were acquired in three-dimension using laboratory-made scanner and single element transducer (center frequency 15 MHz), and were digitized to 12-bits with the sampling frequency of 250 MHz. The scanning pitch was 50 μm. In calculation of the experimental BSC [m^{-1} sr^{-1}], we applied the reflector method [2] using an acrylic board, and compensated attenuation of tissues. The attenuation coefficient of 2.0 dB/(mm·MHz) of a skin dermis tissue was applied in the attenuation compensation function.

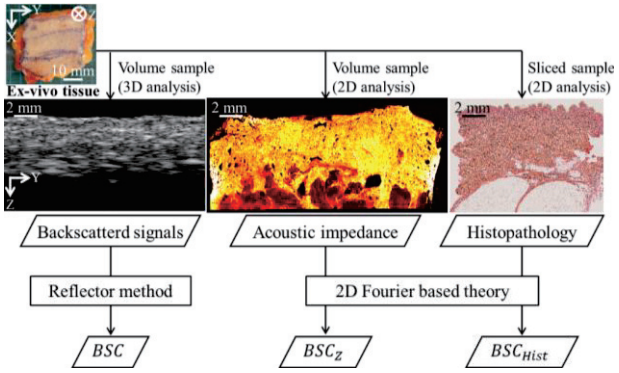

Fig. 1 Comparison of BSCs from three features.

The analysis region for the depth direction was limited from an epidermis to a junction between a dermis and a hypodermis. In this analysis region, the voxel of an analysis window that area was 1.0 mm^3, was shifted in 3-dimension with 50% of overlap.

2.3 Analysis of acoustic impedance

RF echo signals were also measured using scanning acoustic microscopy (modified AMS-50 SI, Honda electronics) with a transducer with the center frequency of 80 MHz. Collected RF echo signals were digitized to 8-bits with the sampling frequency of 2 GHz. The scanning pitch was 16 μm.

Soon after the experiment of Sect. 2.2, each cross-sectional skin sample was mounted on a polystyrene dish, and RF echo signals from the cross-sectional tissue were acquired via purified water and polystyrene dish. The acoustic impedance was computed using the negative peak of RF signals from the boundary of the polystyrene dish - tissue, and that of the purified water - polystyrene dish, respectively.

2.4 Image processing of histopathological image

The specimen was sliced with 10 μm thickness, and was stained with Elastica Van Gieson method. The original unfiltered image was segmented into

†m.omura@chiba-u.jp, *yamaguchi@faculty.chiba-u.jp

collagen fibers, elastin fibers, keratin, and background using superpixels oversegmentation and k-means++ algorithm in Lab color space. The classified pixels of both fibers were assumed as scatterers. The minimum pixel pitch of the digital image was 1 μm.

2.5 Predicting backscatter coefficient

Assuming plane wave propagation, weak scattering in the Born approximation, and that the scatterer medium has spatially random variations of the acoustic impedance and isotropic structure with a 3D radially symmetric function, the predicted BSC is related to the correlation coefficient of the acoustic impedance contrast. The acoustic impedance contrast Z_c was defined as $(Z-\bar{Z})/\bar{Z}$ in the current study, where Z and $\bar{Z}$ is the acoustic impedance of scatterers and surrounding medium. The predicted BSC [m^{-1} rad^{-1}] in k-space [$0{:}\pi/L{:}N\pi/2L$] is defined as [3]

$$BSC(k) = \frac{k^3}{4\pi^2}\overline{\left|\mathcal{F}_{Z_c}(k)\right|^2}\frac{1}{L^2}\left(\frac{L}{N}\right)^4, \quad (1)$$

$$\overline{\left|\mathcal{F}_{Z_c}\right|^2} = \frac{1}{N_L}\sum_{\theta=0}^{\pi/2}\left|\mathcal{F}_{Z_c}(k)_\theta\right|^2, \quad (2)$$

where $|\mathcal{F}_{Zc}|$ is the absolute value of the 2D Fourier transform of the acoustic impedance contrast in each ROI, where θ is angle vector in k-space. N^2 is the pixel size of each ROI. The length L of the square ROI was 1.0 mm^2, and the line number N_L was 100. The radial direction in k-space (wavenumber) equals to the direction of the sound propagation.

The predicated BSCs were calculated from two features: acoustic impedance (Sect. 2.3) and histopathological (Sect. 2.4) based models. To calculate the acoustic impedance contrast, $\bar{Z}$ was assumed to the mean of the acoustic impedance in each ROI. Also in the histopathological based model, Z_c was constantly 0.33 (noted that Z and $\bar{Z}$ are 2.0 and 1.5 Mrayl. respectively) in both fibers pixels.

3. Results

Figure 2 shows the median and 25-75 percentiles of BSCs from backscattered signals and two features. As compared BSCs between LE (−) and LE (+), the median of the experimental BSC in LE (+) was constantly lower (relative difference of

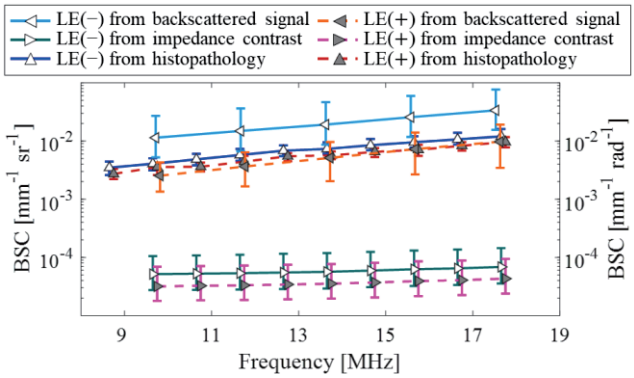

Fig. 2 Calculated BSCs from three features.

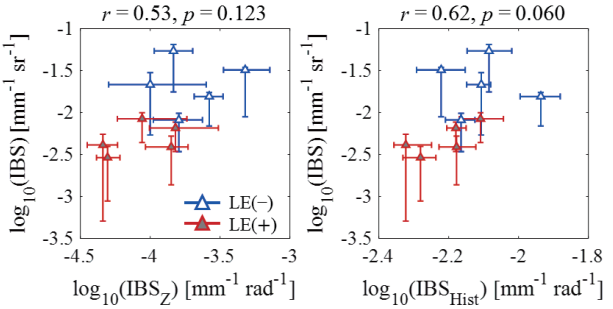

(a) **(b)**

Fig. 3 Relationship of integrated BSCs.

−72%) than that of LE (−) at each frequency. In addition, the predicted BSC_Z and BSC_{Hist} of LE (−) group was lower (−48% and −22%, respectively) than that of LE (+) within the frequency 8−18 MHz, however the larger relative differences (>several 40 dB) were obtained as compared between the BSC and BSC_Z.

Figures 3(a) and **3(b)** display correlation diagrams among integrated BSCs (IBS) of the experimental, acoustic impedance map, and histopathological image. The Spearman rank correlation coefficient r and its p-value were calculated from the medians of all patients. The features of experimental parameters corresponded to those of predicted values; LE (+) groups had lower IBS, IBS_Z, and IBS_{Hist} than LE (−) groups. Also, the experimental IBS is positively correlated to predicted IBS. Our results agree with the relationship between the experimental and predicted ultrasound backscattered properties. It is considered that the macroscopic ultrasound backscattering properties at a center frequency of 15 MHz can be associated with the differences both of the microstructure and acoustic impedance distribution at 80 MHz.

4. Conclusion

The relationship among backscattered signals, acoustic properties, and histopathological structures was confirmed based on the BSC analysis. The difference of the BSC between without and with LE was comparable to predicted BSCs from the acoustic impedance and histopathology. In future works, the form factor will be deduced to model the frequency dependence of the scatterer structure.

Acknowledgment

This work was partly supported by JSPS Core-to-Core Program, and KAKENHI Grant Numbers 17H05280, 19H04482, 17J07762, and Frontier Science Program of Graduate School of Science and Engineering, Chiba University.

References

1. M. Omura et al.: Jpn. J. Appl. Phys. **57** (2018).
2. X. Chen et al.: IEEE Trans. Ultrason. Ferroelectr. Freq. Control **44** (1997).
3. W.H Carter et al.: J. Opt. Soc. Am., **67**, (1977).